

## Experimental Study of Dimethyl Methylphosphonate Decomposition over Anatase TiO<sub>2</sub>

Dmitry A. Trubitsyn and Alexander V. Vorontsov\*

*Boriskov Institute of Catalysis, pr. Ak. Lavrentieva 5, Novosibirsk 630090, Russia*

*Received: July 11, 2005; In Final Form: September 13, 2005*

Removal from air and decomposition of dimethyl methylphosphonate (DMMP) over high surface area anatase TiO<sub>2</sub> at ambient temperature have been quantitatively studied by employing Fourier transform infrared (FTIR) technique under static conditions. In the first scenario of air purification, DMMP underwent reactive adsorption that upon completion was followed by photocatalytic oxidation. DMMP was captured over the TiO<sub>2</sub> surface at the speed of external diffusion. Hydrolysis of adsorbed DMMP led to methanol and methyl methylphosphonate (MMP). At low DMMP coverage quantity, it hydrolyzed completely with the formation of completely surface-bound methanol at 1% relative humidity (RH) and mostly gaseous methanol at 50% RH. Photocatalytic oxidation generated CO<sub>2</sub> as the only carbonaceous gaseous product and bidentate formates as the intermediate surface product. At high DMMP coverage quantity, it was captured incompletely and hydrolyzed partially with CH<sub>3</sub>OH in the gas phase only, 50% RH enhancing both processes. Photocatalytic oxidation generated gaseous HCOOH, CO, and CO<sub>2</sub> and was incomplete due to catalyst deactivation by nonvolatile products. In the second scenario of air purification, DMMP underwent adsorption, hydrolysis, and photooxidation at the same time. It resulted in the quickest removal of DMMP from the gas phase and completion of oxidation in 30 min, suggesting this process for practical air decontamination. At least 0.8 nm<sup>2</sup> of TiO<sub>2</sub> surface per each DMMP molecule should be available for complete purification of air.

### I. Introduction

Recent research on oxide surface science has focused to a great extent on efficient materials for the safe destruction of bulk quantities of chemical warfare agents (CWAs) as well as decontamination of the environment from CWAs after their release including the case of chemical terrorism. Catalyst deactivation is the biggest obstacle in the application of catalytic methods for destroying big quantities of CWAs. However, the good adsorption properties and reactivity of many metal oxides allow application of them for the removal of polar molecules of dilute contaminants and their destruction into safer products.

K. J. Klabunde et al. initiated the research on MgO surface chemistry and its application for the destruction of phosphorus compounds.<sup>1,2</sup> The key to the high reactivity of this catalyst was the thermal activation of MgO having a very high surface area. Chemisorbed molecules of triethyl phosphate, trimethyl phosphate, and dimethyl methylphosphonate (DMMP) started to decompose over MgO even at room temperature.<sup>2</sup> Chemisorption took place via the P=O moiety of phosphate and phosphonate molecules. MgO was also demonstrated to hydrolyze the real CWAs soman, mustard gas, and VX into products of lower toxicity.<sup>3</sup> The decomposition of these liquid CWAs took from above 1 h for soman to more than 25 h for mustard gas and VX.

DMMP is the most often used simulant of phosphorus CWAs for the civilian research environment. Mitchell et al. studied the adsorption and decomposition of DMMP over Al<sub>2</sub>O<sub>3</sub>, MgO, La<sub>2</sub>O<sub>3</sub>, and Fe<sub>2</sub>O<sub>3</sub>.<sup>4</sup> Significant decomposition of chemisorbed DMMP was manifested by the removal of methoxy groups and started after the temperature increased to 100–500 °C. Over Fe<sub>2</sub>O<sub>3</sub>, decomposition of both methoxy and methyl groups was

observable at temperatures above 200 °C. In a later study,<sup>5</sup> it was found that DMMP undergoes reactive adsorption over metal oxide surfaces in a flow reactor even at 25 °C. Methanol and dimethyl ether were the volatile products produced at this temperature. Only 10% of the adsorbed DMMP quantity was converted into these products at 25 °C. Aluminum oxide coimpregnated with cerium and iron oxides was demonstrated to exhibit twice higher activity than the above-mentioned oxides.<sup>6</sup> This coimpregnated system also provided about 10% conversion of DMMP into products.

Oxides of nickel, iron, copper, and vanadium supported over  $\gamma$ -Al<sub>2</sub>O<sub>3</sub> showed activity in DMMP destruction at 400–600 °C.<sup>7</sup> Supported vanadium oxide showed the longest time before deactivation in the removal of DMMP vapors. WO<sub>3</sub> was demonstrated to adsorb DMMP via the P=O moiety on Lewis and Bronsted acid sites at room temperature, but decomposition was not detected.<sup>8</sup> TiO<sub>2</sub> Degussa P25 showed 50% decomposition of adsorbed DMMP by a temperature of 200 °C, but no decomposition was reported to proceed at room temperature.<sup>9</sup>

The challenge of personnel and equipment decontamination limits the temperature and humidity range for CWA destruction to near ambient conditions. Besides, the materials must deliver quick and complete detoxification of adsorbed CWA. The study by Rusu and Yates<sup>10</sup> demonstrated that DMMP adsorbed on a TiO<sub>2</sub> Degussa P25 surface undergoes hydrolysis of methoxy groups at temperatures as low as –59 °C. This observation makes TiO<sub>2</sub> a good candidate for a decontaminating agent, though the conversion of adsorbed DMMP was not measured.

Photoassisted reactions can deliver complete destruction of organic compounds into inorganic products under ambient conditions without additional oxidizers. Amorphous manganese oxide was showed to photocatalytically oxidize DMMP vapors at 70 °C.<sup>11</sup> Oxidation resulted in methylphosphonic acid as the final surface product, thus delivering no complete mineralization.

\* Corresponding author. Phone: 7 383 3331617. Fax: 7 383 3308056. E-mail: voronts@catalysis.nsk.su.

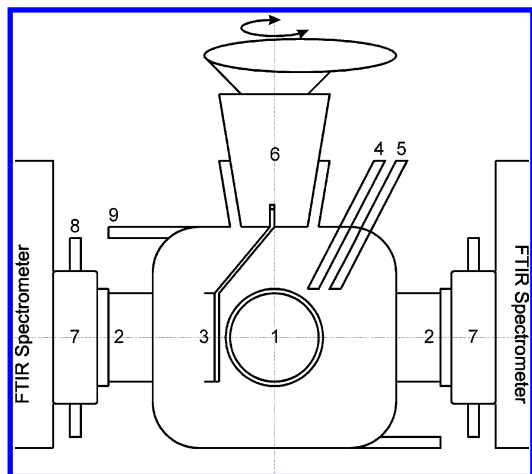


**Figure 1.** IR cell employed for dark and photocatalytic experiments: (1) quartz window; (2) BaF<sub>2</sub> windows; (3) TiO<sub>2</sub> sample in sample holder; (4) heated injector; (5) purge gas input; (6) conical joint; (7) gaseous N<sub>2</sub> purged connectors to FTIR spectrometer; (8) gaseous N<sub>2</sub> inputs and outlets; (9) thermostated water inlet and outlet.

Photocatalytic oxidation over TiO<sub>2</sub> Degussa P25 demonstrated destruction of DMMP into surface phosphate species.<sup>12</sup> The catalyst deactivated due to the accumulation of surface oxidation products, but its activity was completely restored by washing with water. Fourier transform infrared (FTIR) spectroscopic study on DMMP photocatalytic oxidation over TiO<sub>2</sub> Degussa P25 has been performed at  $-73$  °C.<sup>13</sup> All the identified products of oxidation—CO, CO<sub>2</sub>, formate, and water—resided over the catalyst surface at this low temperature. The catalyst deactivated during the process. The applicability of these low temperature results to a decontamination process under ambient conditions is therefore arguable.

In our preliminary study, FTIR in situ technique has been developed and applied for room temperature hydrolysis and photocatalytic oxidation of DMMP over nanocrystalline anatase TiO<sub>2</sub> in a batch reactor.<sup>14</sup> In the present paper, we report in detail the effect of air humidity and DMMP quantity on room temperature DMMP hydrolysis and photocatalytic oxidation chemistry over high surface area anatase TiO<sub>2</sub> powder.

## II. Experimental Methods

**1. FTIR in situ Studies.** Transmission FTIR in situ spectroscopy was the main experimental technique we used. Experiments were carried out in a 300 mL thermostated batch reactor mounted in the cell compartment of a spectrometer (Vector 22, Bruker), as shown in Figure 1. The temperature of the reactor was kept equal to 300 K throughout all experiments.

The front window (1) was made of quartz, transparent for UV light, while the side windows (2) were made of barium fluoride transparent for the IR beam.

The TiO<sub>2</sub> sample (3) can be placed in two different positions. In the first one, the sample is exposed to UV light and does not cover the IR beam so that the IR spectra of gaseous species can be measured. In the second position, the sample covers the IR beam. The location of the sample can easily be changed during one experiment as many times as needed without opening the reactor.

The TiO<sub>2</sub> used was Hombifine N produced by Sachtleben Chemie GmbH, which is reported to have 100% anatase composition and a surface area of 340 m<sup>2</sup>/g. The TiO<sub>2</sub> samples were prepared by the following procedure. TiO<sub>2</sub> powder (150 mg) and ultraclean water (5 mL) obtained with a Barnstead Easypure II RF device were blended in a closed vial and treated

in an ultrasound bath (UZV-1/100-TN, 25 kHz) for 15 min. After that, 200  $\mu$ L of the acquired aqueous suspension was deposited on the round calcium fluoride substrate and dried out at room temperature. The surface density of deposited TiO<sub>2</sub> was 2 mg/cm<sup>2</sup>, and the total TiO<sub>2</sub> mass was 6 mg, which corresponds to a surface area of about 2 m<sup>2</sup>. For the (001) and (100) anatase surfaces, this corresponds to about 23.7 and 18.9  $\mu$ mol of surface Ti atoms, respectively, and 21  $\mu$ mol on average.

Before the experiments, the samples were exposed to UV light in the flow of clean air at room temperature to remove small amounts of organic contamination from the TiO<sub>2</sub> surface. This pretreatment lasted several hours and ceased after the IR spectrum finished changing.

A mercury lamp (DRSh-1000) was used for UV irradiation. UV light was focused on the TiO<sub>2</sub> sample so that the bright UV spot had the same size and shape as the round TiO<sub>2</sub> sample. The UV light ( $\lambda < 390$  nm) intensity at the photocatalyst surface was about 0.2 W/cm<sup>2</sup>. The quantity of oxygen inside the IR cell was 2600  $\mu$ mol, whereas the quantity of oxygen for complete oxidation of the maximum DMMP quantity used in the experiments (45  $\mu$ mol) was 225  $\mu$ mol. Thus, enough oxygen was present for complete DMMP mineralization and no crucial oxygen concentration change took place in the photocatalytic experiments.

The reactor was equipped with the injector (4) heated to 160 °C, which allowed evaporating injected liquid DMMP in less than 2 min. DMMP (97%) was obtained from Aldrich.

The reactor was connected to a clean air source through the channel (5) so that clean air could pass through the reactor at a velocity of 300 mL/min. Air was cleaned and dried out by two consecutive blocks. The first one was sequentially filled up with NaX zeolite, activated charcoal, and silica gel. The second block was filled up with the mixture of activated charcoal and sodium hydroxide to remove CO<sub>2</sub>.

Water vapor and gaseous carbon dioxide present in atmospheric air could interfere with the spectra of interest. Therefore, the IR beam outside the reactor was isolated from atmospheric air with two Teflon flanges (7) purged with gaseous nitrogen.

**2. Analysis of IR Spectra.** All the reported IR spectra present the changes that happened in the reactor relative to the initial state. In that way, an area under the spectrum of any substance determines the difference between the final and initial quantity of this substance in the reactor.

The concentration of CO<sub>2</sub> in the reactor was measured by comparing the area under the  $\nu_a(\text{CO})$  bands (2240–2400 cm<sup>-1</sup>) with the corresponding calibration curve obtained in a separate experiment. Similarly, CO concentration was determined using the  $\nu(\text{CO})$  band (2005–2235 cm<sup>-1</sup>) area.

The concentrations of all the other gaseous compounds were determined by the following procedure. Spectra of a given amount of all compounds that appear in the course of hydrolysis or photooxidation of DMMP were separately measured. Then, the spectrum to be analyzed was approximated with the sum of the scaled spectra of all compounds to obtain the best fit. Concentrations of corresponding compounds were determined using obtained scale factors.

The amount of adsorbed methanol was determined from the height of the  $\nu_s(\text{CH})$  band (2830 cm<sup>-1</sup>), which was determined as the length of the vertical line h segment, confined between the top of the band and tangent t (see Figure 2).

## III. Results and Discussion

The present research aims at investigation of DMMP destruction under conditions close to ambient. Variations in organics

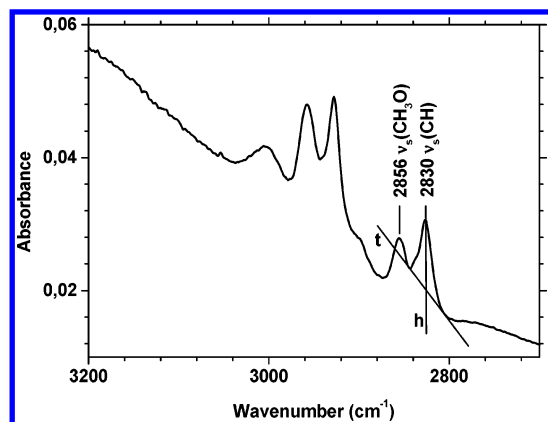


**Figure 2.** Method of separation of adsorbed DMMP and methanol bands and measurement of adsorbed methanol band height.

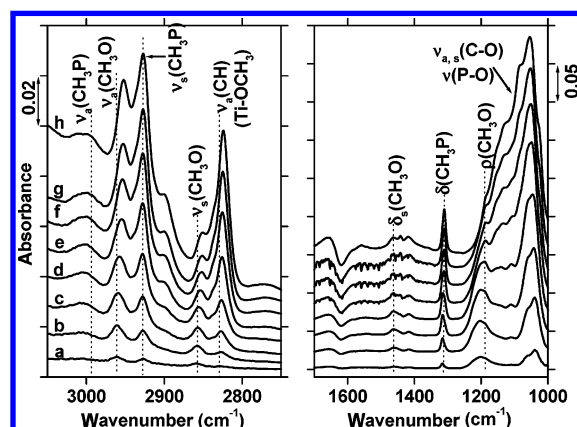


**Figure 3.** Transmission FTIR spectra of adsorbed species during reactive adsorption of a low coverage quantity of DMMP at 1% relative humidity. Time after evaporation of DMMP: (a) 1 min; (b) 5 min; (c) 15 min; (d) 41 min; (e) 75 min; (f) 195 min; (g) 375 min; (h) 1320 min.

concentration and air humidity can strongly affect hydrolysis and photocatalytic oxidation.<sup>15,16</sup> There are two possible scenarios for destruction under ambient conditions that are considered below: (1) hydrolysis followed by photocatalytic oxidation and (2) simultaneous hydrolysis and photocatalytic oxidation. The separate steps of these two scenarios are considered in the following subsections.

**1. Reactive Adsorption at Submonolayer DMMP Surface Coverage and 1% Relative Humidity.** Decomposition was first performed at a low air relative humidity of 1%. A 0.9  $\mu\text{mol}$  portion of liquid DMMP that corresponds to a  $\text{TiO}_2$  sample surface coverage well below monolayer was injected into the heated injection port of the FTIR cell. Complete evaporation of liquid DMMP takes less than 2 min. The evaporation time was measured in a blank experiment in the absence of photocatalyst. The IR spectrum of the gas-phase DMMP was identical to the previously reported spectrum.<sup>10</sup> After the evaporation, the gas-phase DMMP concentration decreased to below the spectrometer detection limit (approximately 3 ppm) in 40 min. No gaseous products of hydrolysis were detected during this experiment. The FTIR spectra of the  $\text{TiO}_2$  surface are presented in Figure 3.

The titanium dioxide used in the experiments was not thermally treated, and therefore, its surface is strongly hydroxylated. This causes the IR spectrum of adsorbed DMMP to be significantly different from the reported spectra over annealed oxides that were used for the low temperature experiments.<sup>1,2,10</sup> The  $\nu(\text{P}=\text{O})$  band found for gaseous DMMP at  $1276\text{ cm}^{-1}$  and

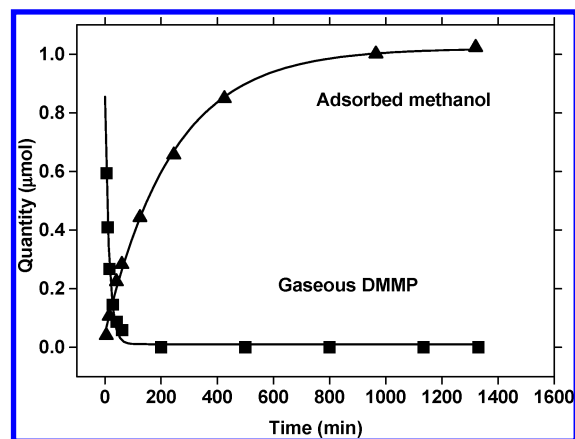


**Figure 4.** Profiles of quantities of gaseous DMMP and adsorbed methanol during reactive adsorption of 0.9  $\mu\text{mol}$  of DMMP at 1% relative humidity.

condensed/adsorbed DMMP at  $1242\text{ cm}^{-1}$  shifts in our case to a lower frequency and merges with the  $\rho(\text{CH}_3\text{O})$  vibration to form the wide band around  $1200\text{ cm}^{-1}$ . It was reported earlier that interaction of the  $\text{P}=\text{O}$  moiety of DMMP with surface hydroxyl groups causes the shift of the  $\nu(\text{P}=\text{O})$  band to  $1210\text{ cm}^{-1}$ .<sup>10</sup> Such interaction can also give input to the observed spectra of adsorbed DMMP in Figure 3. One can see in the CH stretching vibration region ( $3000\text{--}2800\text{ cm}^{-1}$ ) that the intensity of the adsorbed DMMP bands<sup>10</sup> increases with time of experiment due to the accumulation of DMMP and its hydrolysis product on the  $\text{TiO}_2$  surface. The band  $\nu_a(\text{CH})$  of adsorbed methanol at  $2828\text{ cm}^{-1}$  appears shortly after the start of DMMP adsorption and corresponds to surface-bound methoxy groups.<sup>10</sup> The appearance of the methanol testifies to reactive adsorption of DMMP. In addition to the appearance of the methanol band and the shift of the  $\nu(\text{P}=\text{O})$  band, the position of the  $\nu_a(\text{CH}_3\text{O})$  band of DMMP shifts from  $2961$  to  $2951\text{ cm}^{-1}$  and new bands appear at  $2902$  and  $1418\text{ cm}^{-1}$ . The latter band can be assigned to  $\delta_s(\text{CH}_3\text{O})$  vibrations. Thus, reactive adsorption of DMMP induces strong interaction of  $\text{P}=\text{O}$  and  $\text{P}-\text{O}-\text{CH}_3$  moieties with the surface and possibly several types of adsorption of products. The formation of the negative band at  $1620\text{ cm}^{-1}$  indicates consumption of adsorbed water molecules in the course of DMMP hydrolysis.

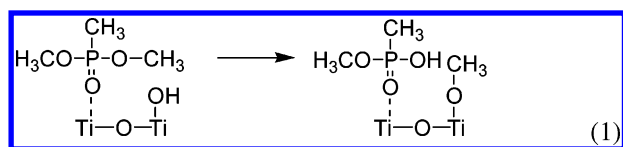
The band of adsorbed methanol at  $2828\text{ cm}^{-1}$  is relatively well separated from the  $\nu_s(\text{CH}_3\text{O})$  band of adsorbed DMMP to allow calibration for the adsorbed methanol quantity. Figure 4 shows how the DMMP quantity in the gas phase decreases and the amount of adsorbed methanol rises in the course of the experiment. Both kinetic curves obey the exponential law. The first-order rate coefficient of the DMMP concentration decay is  $7.1 \times 10^{-2}\text{ min}^{-1}$ , and that for the methanol formation is  $4.2 \times 10^{-3}\text{ min}^{-1}$ . Methanol capture was 90% completed after 42 min of reaction, while hydrolysis was 90% completed after 500 min. Thus, the major quantity of adsorbed methanol forms after most of the DMMP is already captured from the gas phase. The first two or three spectra in Figure 3 represent mainly adsorbed unreacted DMMP. This is consistent with the absence of the shift of the  $\nu_a(\text{CH}_3\text{O})$  band of DMMP and the absence of bands of the  $\text{P}-\text{O}_x$  moiety of hydrolyzed DMMP in the  $1000\text{--}1200\text{ cm}^{-1}$  region in these initial spectra.

The total amount of adsorbed methanol formed in DMMP reactive adsorption is  $1\text{ }\mu\text{mol}$ , which is within experimental error (10%) equal to the initial amount of DMMP. Rusu and Yates<sup>10</sup> supposed that hydrolysis of DMMP over a  $\text{TiO}_2$  surface proceeds via elimination of a single  $\text{CH}_3\text{O}$  group from the

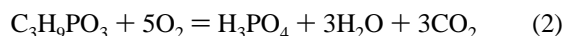


DMMP molecule. Our quantitative results on methanol formation kinetics are in agreement with this hypothesis. However, there are chances that some quantity of DMMP could undergo hydrolysis on both  $\text{CH}_3\text{O}$  groups, whereas some DMMP stays unhydrolyzed. To check the possibility of the second stage hydrolysis, we washed the  $\text{TiO}_2$  with water after reactive adsorption of DMMP in a separate experiment. The FTIR spectrum of the  $\text{TiO}_2$  after the washing demonstrated complete disappearance of C–H stretch vibration bands, indicating thereby the complete removal of the hydrolysis products. Identification of DMMP hydrolysis products was done following the published derivatization procedure and GC-MS analysis.<sup>16</sup> Only methyl methylphosphonic acid (MMP) and methanol were detected in the wash water. This provides the final evidence for hydrolysis to proceed only at a single methoxy group of DMMP. In the present experiment, all adsorbed molecules of DMMP underwent hydrolysis.

Experimental and literature data allow us to suggest the following mechanism of reactive adsorption for DMMP (eq 1).



**2. Photocatalytic Oxidation after Completion of Reactive Adsorption at Submonolayer DMMP Surface Coverage and 1% Relative Humidity.** After reactive adsorption was finished, we started irradiating the sample of the  $\text{TiO}_2$  with adsorbed products of hydrolysis. The gas-phase  $\text{CO}_2$  concentration started increasing immediately after the start of irradiation. The  $\text{CO}_2$  concentration increase was well approximated by the exponential law with the first-order rate coefficient  $0.29 \text{ min}^{-1}$ . The initial rate of  $\text{CO}_2$  formation was  $7.6 \times 10^{-7} \text{ mol/s}$ . The reaction was 90% completed in 10 min after the start of irradiation. The total quantity of the formed  $\text{CO}_2$  was  $2.8 \text{ } \mu\text{mol}$ , which corresponds to triple the amount of initial DMMP within experimental error. Thus, DMMP underwent complete destruction into inorganic products at the end of this experiment according to the following equation.



Changes in surface species during photocatalytic oxidation of hydrolyzed DMMP are demonstrated in Figure 5. Several new bands appeared after the start of irradiation. Comparison with the spectrum of adsorbed formic acid (curve h in Figure 5) reveals that the new bands correspond to adsorbed formic acid. The bands of adsorbed formic acid are listed in Table 1. It should be noted that the observed spectrum of adsorbed formic acid for the present anatase  $\text{TiO}_2$  sample is significantly different from the reported spectrum over the anatase + rutile Degussa P25 sample.<sup>17</sup> The absence of the formic acid  $\nu(\text{C}=\text{O})$  bands at approximately  $1675 \text{ cm}^{-1}$  allows us to conclude that formic acid is adsorbed as surface formates. The difference between the asymmetric and symmetric modes of  $\nu(\text{COO})$  of adsorbed formic acid corresponds to the bridging geometry of formates; that is, oxygens are coordinated to different Ti surface atoms.<sup>18</sup>

Bands of adsorbed MMP and methanol decrease during the oxidation process. Oxidation preferentially proceeds first at the methoxy group of MMP and methanol rather than at the methyl group. This follows from consideration of the spectrum resulting from subtracting the scaled spectrum of adsorbed formic acid from the spectra of adsorbed species. The  $\text{CH}_3\text{P}$  group band is present for a longer time in these subtracted IR spectra and

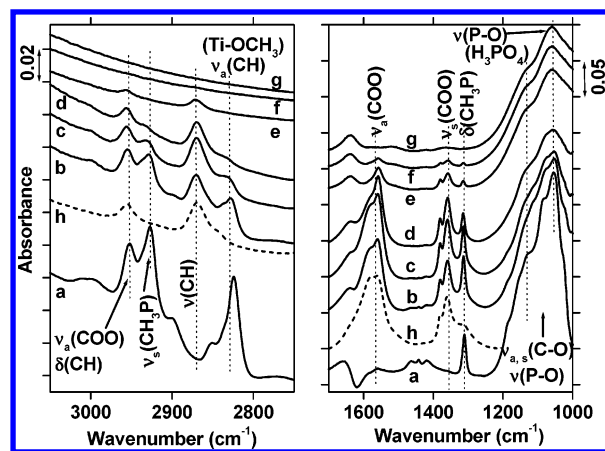


**Figure 5.** FTIR spectra of the surface species during photocatalytic oxidation of  $0.9 \text{ } \mu\text{mol}$  of hydrolyzed DMMP at 1% relative humidity. Time after the start of irradiation: (a) 0 min; (b) 1 min; (c) 2 min; (d) 4 min; (e) 10 min; (f) 14 min; (g) 30 min. (h) Spectrum of adsorbed formic acid in a quantity of  $2.5 \text{ } \mu\text{mol}$  ( $0.83 \text{ } \mu\text{mol/cm}^2$ ).

**TABLE 1: Assignment of Bands of Formic Acid Formed in Photocatalytic Oxidation of DMMP**

entry no.	wavenumber, $\text{cm}^{-1}$	assignment
1	2955	$\delta(\text{CH}) + \nu_{\text{a}}(\text{COO})$
2	2870	$\nu(\text{CH})$
3	1577	$\nu_{\text{a1}}(\text{COO})$
4	1560	$\nu_{\text{a2}}(\text{COO})$
5	1380	$\nu_{\text{s1}}(\text{COO})$
6	1358	$\nu_{\text{s2}}(\text{COO})$
7	1311	$\delta(\text{CH})$

obviously is more resistant to oxidation than  $\text{CH}_3\text{O}$  moieties. Adsorbed formic acid, an intermediate product of oxidation, is oxidized in the last stage of the reaction. Water and phosphoric acid are the final surface products of oxidation with bands at  $1638$  and  $1057 \text{ cm}^{-1}$ , respectively.

**3. Reactive Adsorption at Submonolayer DMMP Surface Coverage and 50% Relative Humidity.** To determine the effect of humidity, reactive adsorption was performed at 50% air relative humidity. After evaporation of injected DMMP, its concentration in the gas phase decreased to below detection threshold ( $\sim 3 \text{ ppm}$ ) in 60 min. The concentration versus time curve is fitted by exponential decay with the first-order rate coefficient  $5.0 \times 10^{-2} \text{ min}^{-1}$ . In contrast to the experiment at low air humidity, the formation of gas-phase methanol was observed. The concentration versus time curve for gas-phase methanol obeyed exponential law with the first-order rate coefficient  $3.6 \times 10^{-3} \text{ min}^{-1}$ . The initial rate of methanol formation was  $4.7 \times 10^{-9} \text{ mol s}^{-1}$ . After completion of hydrolysis, the amount of gas-phase methanol was equal to the initial amount of injected DMMP within experimental error. Evidently, methanol was displaced from the  $\text{TiO}_2$  surface into the gas phase by large amounts of water present in the system.

Figure 6 shows FTIR spectra of  $\text{TiO}_2$  during reactive adsorption. The positions and assignment of bands in these spectra are similar to those in Figure 3. The intensity of bands in the high frequency region is much lower at 50% humidity than at 1% humidity. This is probably connected with interaction of DMMP and hydrolysis product MMP with adsorbed water. The band of adsorbed methanol has especially low intensity due to removal of methanol into the gas phase. Appearance of the band at  $1570 \text{ cm}^{-1}$  is attributable to the change of the state of adsorbed water due to interaction with the product of DMMP hydrolysis.

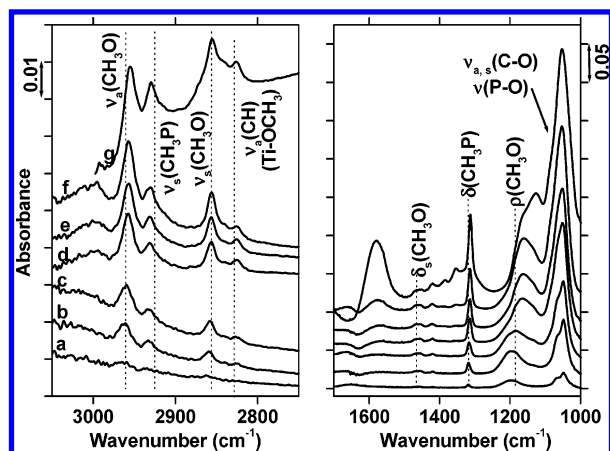


**Figure 6.** Transmission FTIR spectra of adsorbed species during reactive adsorption of DMMP at a low coverage quantity and a relative humidity of air of 50%. Time after evaporation of DMMP: (a) 1 min; (b) 8 min; (c) 20 min; (d) 60 min; (e) 90 min; (f) 225 min; (g) 1310 min.

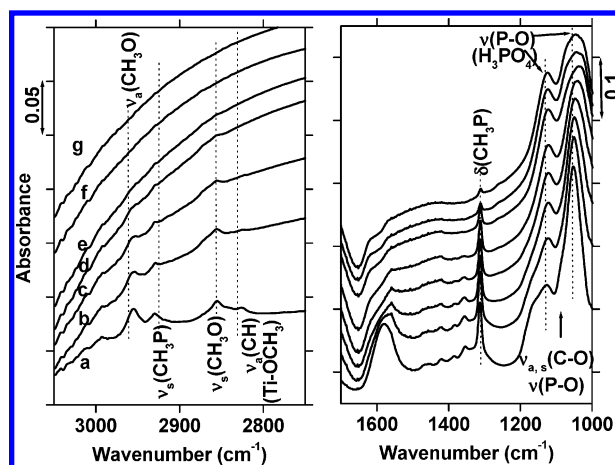


**Figure 7.** Transmission FTIR spectra of adsorbed species during photocatalytic oxidation of DMMP hydrolysis products at a low DMMP coverage quantity and 50% relative humidity. Time after the start of irradiation: (a) 0 min; (b) 1 min; (c) 4 min; (d) 8 min; (e) 13 min; (f) 30 min; (g) 50 min.

**4. Photocatalytic Oxidation after Completion of Reactive Adsorption at Submonolayer DMMP Surface Coverage and 50% Relative Humidity.** After starting irradiation of the TiO<sub>2</sub> sample in the IR cell, the concentration of gas-phase CO<sub>2</sub> started increasing. The CO<sub>2</sub> concentration profile was approximated by the exponential law with the first-order rate coefficient 0.25 min<sup>-1</sup>. The initial rate of the CO<sub>2</sub> formation was 6.7 × 10<sup>-7</sup> mol s<sup>-1</sup>. The concentration of the gas-phase methanol decreased according to the exponential law with the first-order reaction rate coefficient 0.33 min<sup>-1</sup>. The oxidation reaction proceeded until complete consumption of organic molecules and formation of CO<sub>2</sub> in a quantity corresponding to the initial quantity of carbon in the system.

Changes of IR spectra of the photocatalyst surface during oxidation are shown in Figure 7. Due to the heating of the TiO<sub>2</sub> sample under irradiation, there is a negative band of adsorbed water in these spectra. Compared to the previous experiment at low air humidity, the intensity of all bands decreased due to the interactions with large quantities of adsorbed water. Formic acid was not detected also due to strong interaction with the polylayers of adsorbed water. The final surface product of oxidation, phosphoric acid, exhibits a distorted spectrum with two separate bands at 1048 and 1123 cm<sup>-1</sup>.

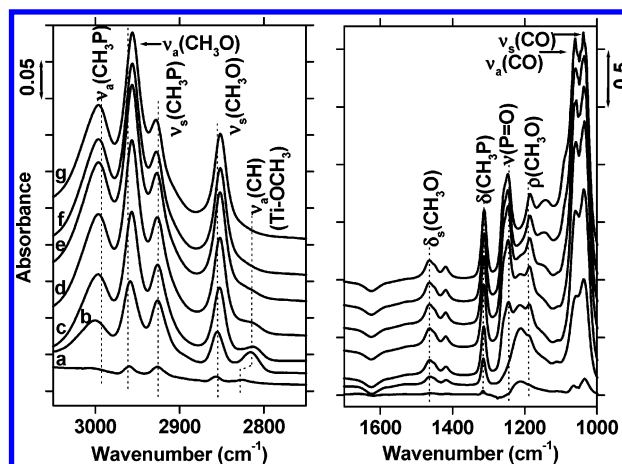


**Figure 8.** Transmission FTIR spectra of surface species during reactive adsorption of a high coverage quantity of DMMP at 1% air relative humidity. Time after DMMP evaporation: (a) 1 min; (b) 4 min; (c) 8 min; (d) 12 min; (e) 40 min; (f) 220 min; (g) 1096 min.

### 5. Reactive Adsorption at High DMMP Surface Coverage and 1% Relative Humidity.

The next stage of the present research is devoted to the interaction of the TiO<sub>2</sub> surface with DMMP in a quantity of 45 μmol that corresponds to coverage significantly exceeding monolayer. After injection and evaporation of DMMP in the IR cell, its gas-phase concentration decreased according to the exponential law with the rate coefficient 7.2 × 10<sup>-2</sup> min<sup>-1</sup>. However, the DMMP concentration did not fall to zero but stabilized at the level corresponding to 12 μmol. At the same time, the concentration of gas-phase methanol increased according to the exponential law with the rate coefficient 2.7 × 10<sup>-2</sup> min<sup>-1</sup> and the initial rate 2.2 × 10<sup>-8</sup> mol s<sup>-1</sup>. The methanol quantity in the gas phase reached a maximum value of 1.8 μmol and did not grow thereafter. The rate of DMMP removal was again much higher than the rate of methanol formation in the hydrolysis reaction. These observations indicate that the quantity of DMMP used in this experiment was too large for complete hydrolysis over the given quantity of TiO<sub>2</sub>. The quantity of adsorbed DMMP was 5.5 μmol/mg of TiO<sub>2</sub>, whereas the number of surface Ti atoms approximates 3.5 μmol/mg of TiO<sub>2</sub>. In reality, adsorption of every DMMP molecule requires more than one surface Ti atom, since the DMMP adsorption area is about 0.4 nm<sup>2</sup> and the area for each surface Ti atom is only about 0.16 nm<sup>2</sup>. Therefore, adsorption of DMMP proceeded with the formation of polylayers. Only every fifth adsorbed DMMP molecule underwent hydrolysis.

The surface changes during the reactive adsorption are exhibited by the FTIR spectra shown in Figure 8. Adsorbed methanol is observed over the photocatalyst surface only for the first 12 min of reaction. Thereafter, it is completely displaced into the gas phase by adsorbing DMMP or its hydrolysis product MMP. The shape of the spectrum in the low frequency region is markedly different from spectra measured at a low coverage of DMMP.

After 8 min of reaction, the spectrum of adsorbed DMMP almost completely coincides with the spectrum of liquid DMMP<sup>19</sup> exhibiting absorption bands at 2996, 2956, 2952, 2927, 1465, 1420, 1313, 1245, 1188, and 1037 cm<sup>-1</sup>. This confirms the polylayer nature of the adsorbed DMMP molecules with weak interaction with the TiO<sub>2</sub> surface. This spectrum also corresponds to the majority of spectra reported for hydrolysis of DMMP over TiO<sub>2</sub> Degussa P25,<sup>10</sup> suggesting that the authors of this work used high surface coverages of DMMP and obtained a low conversion of DMMP into its hydrolysis products.

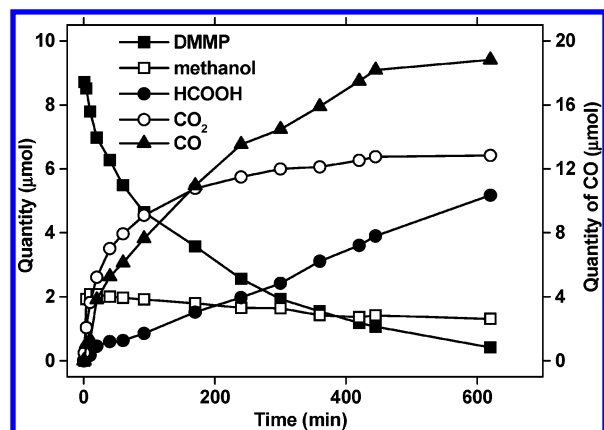


**Figure 9.** Quantities of gas-phase products formed during photocatalytic oxidation of a high coverage quantity of DMMP at 1% air relative humidity. The total quantity of products after 600 min was 22.3  $\mu\text{mol}$ , which corresponds to a TON of about 1.

**6. Photocatalytic Oxidation after Completion of Reactive Adsorption at High DMMP Surface Coverage and 1% Relative Humidity.** Starting the irradiation of the  $\text{TiO}_2$  sample with adsorbed DMMP and hydrolysis products in both the gas phase and over the surface initiates oxidative processes resulting in several gas-phase products. These products comprise formic acid, carbon monoxide, carbon dioxide, and water. This contrasts with the photocatalytic oxidation at low DMMP surface coverage that resulted in gaseous carbon dioxide and water only. Evidently, the gas-phase products were formed due to the insufficient number of sites to host DMMP and all products of its decomposition over the  $\text{TiO}_2$  surface. Profiles of detected gaseous product quantities were measured using IR spectra of the gas phase and are presented in Figure 9.

The concentration of the gas-phase DMMP undergoes a decrease, which is fitted by exponential decay with the first-order rate coefficient  $6.5 \times 10^{-3} \text{ min}^{-1}$ . The growth of the  $\text{CO}_2$  concentration is well fitted by the exponential law with the first-order rate coefficient  $1.7 \times 10^{-2} \text{ min}^{-1}$  and the initial rate  $2.5 \times 10^{-7} \text{ mol s}^{-1}$ . One can see that the  $\text{CO}_2$  quantity stabilizes at around 6  $\mu\text{mol}$  and does not grow anymore, which signifies photocatalyst deactivation toward complete oxidation. However, products of incomplete oxidation such as formic acid and carbon monoxide form during the whole reaction observation time. Carbon monoxide is the major product of the oxidation reaction. Its final quantity by far exceeds the quantity of any other product and accounts for about half of all carbon in the system.

The changes of surface species during photocatalytic oxidation are represented by the infrared spectra of the surface in Figure 10. Despite big quantities of gaseous products, they are not present over the surface in notable quantities.

In particular, bands of adsorbed formic acid are completely absent in Figure 10. Large quantities of DMMP present in the system effectively displace all nonvolatile products from the surface. The spectrum of adsorbed DMMP undergoes quick changes after the start of irradiation. The  $\nu(\text{P}=\text{O})$  band at  $1247 \text{ cm}^{-1}$  disappears after 10 min. During this time, however, quantities of products formed and DMMP consumed from the gas phase correspond to only a few percent conversion. Therefore, the disappearance of the  $\nu(\text{P}=\text{O})$  band is not associated with transformation of DMMP to products but rather with structural rearrangement of the adsorbed DMMP molecules under irradiation to bring them from a polylayer liquidlike state into the state similar to monolayer (Figure 3).

**7. Reactive Adsorption at High DMMP Surface Coverage and 50% Relative Humidity.** After completion of the evapora-

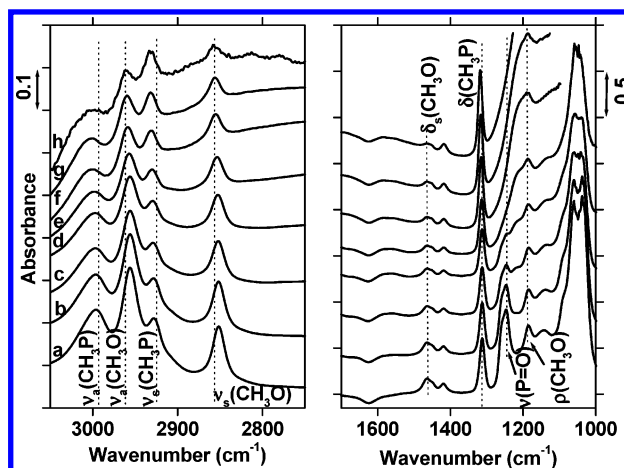


**Figure 10.** Transmission FTIR spectra of surface species during photocatalytic oxidation after reactive adsorption of a high coverage quantity of DMMP at 1% air relative humidity. Time after starting irradiation: (a) 0 min; (b) 1 min; (c) 4 min; (d) 10 min; (e) 40 min; (f) 170 min; (g) 300 min; (h) 620 min.

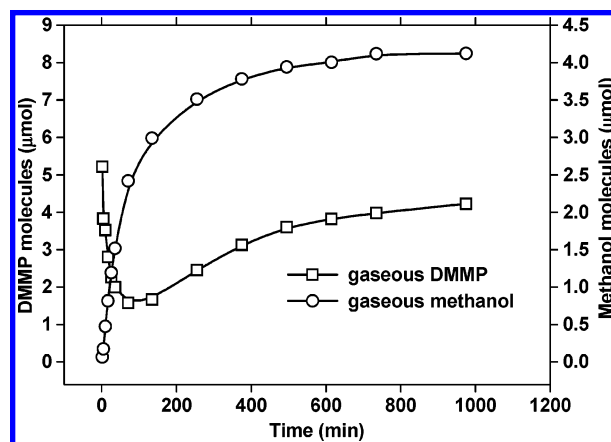


**Figure 11.** Change of gas-phase DMMP and methanol quantities during reactive adsorption of a high surface coverage quantity of DMMP at 50% air relative humidity.

tion of DMMP injected into the reactor in a quantity of 45  $\mu\text{mol}$ , its concentration in the gas phase started decreasing due to the adsorption over the photocatalyst surface. However, after 71 min of reaction, the quantity of gaseous DMMP reached a minimum of 1.6  $\mu\text{mol}$  and started increasing to reach 4.2  $\mu\text{mol}$  after 975 min. The observed profiles of gaseous DMMP and methanol quantities are demonstrated in Figure 11.

The quantity of gaseous methanol steadily increases according to the exponential law with the first-order rate coefficient  $1.2 \times 10^{-2} \text{ min}^{-1}$  and the initial rate  $4.2 \times 10^{-8} \text{ mol s}^{-1}$ . The gaseous methanol quantity reaches 4.1  $\mu\text{mol}$  after 975 min of reaction. This methanol quantity is more than twice larger than the methanol quantity released in hydrolysis of the same DMMP quantity at low air humidity. Water is one of the reagents for the DMMP hydrolysis reaction. Evidently, the water deficit stopped hydrolysis of high DMMP coverages in the low humidity case.

FTIR spectra of the  $\text{TiO}_2$  surface species are shown in Figure 12 for the course of DMMP reactive adsorption. The spectra are similar to the spectra obtained for reactive adsorption at a low humidity level. However, the  $\nu(\text{P}=\text{O})$  band at  $1233 \text{ cm}^{-1}$  appears in the present case significantly later and shows much smaller intensity. It infers that this band appears only after completion of the hydrolysis reaction when DMMP forms polylayer coverages constructed similarly to liquid DMMP.



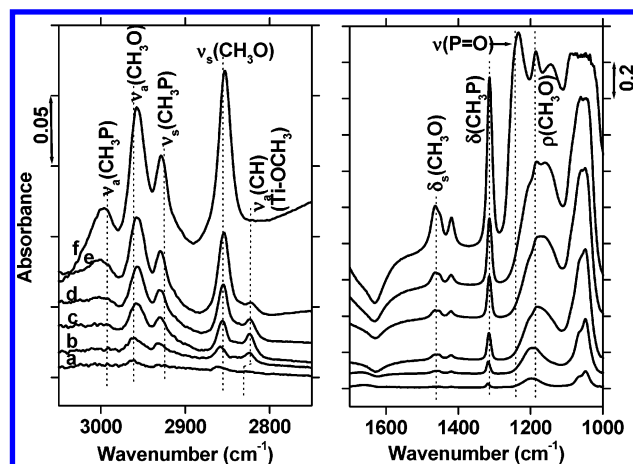


**Figure 12.** Transmission FTIR spectra of surface species during reactive adsorption of a high coverage quantity of DMMP at 50% air relative humidity. Time after DMMP evaporation: (a) 1 min; (b) 4 min; (c) 16 min; (d) 35 min; (e) 70 min; (f) 1061 min.

Another feature of the spectra is the increase of the intensity of the negative band of water at  $1630\text{ cm}^{-1}$  as the hydrolysis reaction proceeds. This indicates consumption of adsorbed water for the production of gas-phase methanol and adsorbed MMP molecules. The fact that the  $\text{TiO}_2$  surface is able to adsorb about  $8\text{ }\mu\text{mol}$  more DMMP at 50% relative humidity than at 1% relative humidity indicates that adsorbed DMMP is partly dissolved in polylayer water surface coverage at high humidity. As the hydrolysis reaction proceeds, about  $4\text{ }\mu\text{mol}$  of water is removed from the  $\text{TiO}_2$  surface in hydrolysis products. This results in desorption of about  $2.6\text{ }\mu\text{mol}$  of DMMP from the photocatalyst surface (Figure 11).

**8. Photocatalytic Oxidation after Completion of Reactive Adsorption at High DMMP Surface Coverage and 50% Relative Humidity.** Starting irradiation of the  $\text{TiO}_2$  sample initiated oxidative reactions that produced the same set of gas-phase products that was observed in photocatalytic oxidation at high DMMP quantity and 1% RH (section 6). The curves of gas-phase product concentrations also have very similar shapes, but the concentrations were a little smaller. The  $\text{CO}_2$  kinetic curve obeys the exponential law with the first-order rate coefficient  $1.5 \times 10^{-2}\text{ min}^{-1}$  and an initial rate of  $\text{CO}_2$  generation of  $1.9 \times 10^{-7}\text{ mol s}^{-1}$ . The  $\text{CO}_2$  quantity grew up to a level of  $5\text{ }\mu\text{mol}$  which is slightly smaller than that in the case of 1% RH. The quantity of gas-phase products at 550 min of irradiation corresponded to conversion of  $9\text{ }\mu\text{mol}$  of DMMP into phosphoric acid. This quantity is slightly smaller than DMMP conversion at 1% RH ( $10\text{ }\mu\text{mol}$ ). A similar negative effect of air humidity on heteroatom organics conversion was previously reported for photocatalytic degradation of diethyl sulfide, an HD simulant, at a light intensity of  $11\text{ mW/cm}^2$ .<sup>20</sup> The value of DMMP conversion of about  $10\text{ }\mu\text{mol}$  into phosphoric acid corresponds to the adsorption of each phosphoric acid molecule over two surface Ti atoms.

Surface species changes during the photocatalytic oxidation and their interpretations are similar to those depicted in Figure 10. Analogous to the photocatalytic oxidation at a low coverage quantity of DMMP (sections 2 and 4), the intensity of high frequency vibrations is smaller at 50% RH.

**9. Simultaneous Hydrolytic and Photocatalytic Decomposition at Submonolayer DMMP Surface Coverage and 1% Relative Humidity.** The alternative method for removal of DMMP from the gas phase and its complete destruction comprises carrying out photocatalytic oxidation immediately

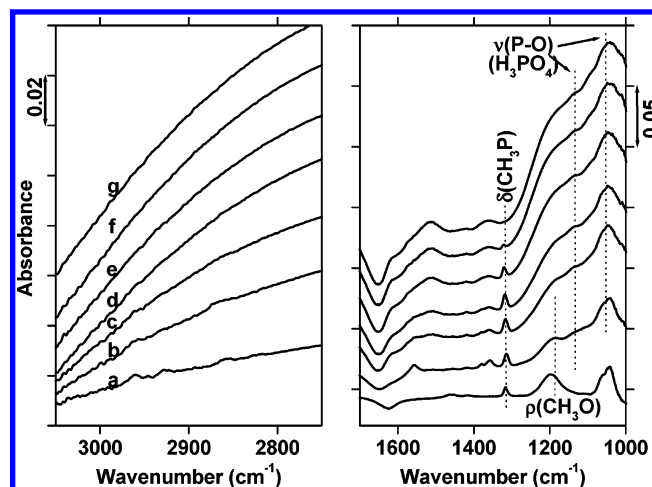


**Figure 13.** Transmission FTIR spectra of surface species during simultaneous reactive adsorption and photocatalytic oxidation of a low coverage quantity of DMMP at 1% air relative humidity. Time after evaporation of DMMP: (a) 1 min; (b) 4.5 min; (c) 8.2 min; (d) 12.2 min; (e) 19.2 min; (f) 33.3 min; (g) 61 min.

after evaporation of the injected DMMP. Adsorption, hydrolysis, and photocatalytic oxidation would proceed simultaneously in this method, which was tested in the present work for a low coverage quantity of DMMP.

To perform the test,  $0.9\text{ }\mu\text{mol}$  of liquid DMMP was injected and evaporated in the IR cell. Irradiation of the  $\text{TiO}_2$  sample was started about 30 s after injection of the liquid DMMP. The concentration of the gas-phase DMMP decreased to below the FTIR spectrometer sensitivity (3 ppm) in about 15 min. The DMMP concentration profile approximated exponential decay with the first-order rate coefficient  $0.28\text{ min}^{-1}$ . The  $\text{CO}_2$  concentration profile also obeyed the exponential law with the rate coefficient  $0.13\text{ min}^{-1}$ . The final  $\text{CO}_2$  quantity was equal to triple the initial quantity of DMMP within experimental error, indicating complete destruction of DMMP into inorganic products.

The surface species during the reaction are revealed by the surface FTIR transmission spectra shown in Figure 13. When compared with consecutive hydrolysis and photocatalytic oxidation represented in Figures 3 and 4, one can see that the intensity of the C–H valent vibrations is much smaller in the present case. This shows that a much smaller amount of organic compounds is present over the photocatalyst surface. After 33 min of irradiation, the reaction can be considered as completed: only phosphoric acid resides over the photocatalyst surface.

Removal of DMMP from the gas phase proceeds via several consecutive stages: (1) transport of DMMP vapor-phase molecules to the photocatalyst sample external surface; (2) transport of DMMP molecules inside the photocatalyst pores to the surface sites; and (3) adsorption of DMMP over free surface sites.

The rates of the two stages of DMMP transport can be readily estimated. The DMMP gas-phase diffusion coefficient ( $D_g$ ) is expressed as

$$D_g = \frac{1}{3} \lambda \langle U \rangle = \frac{1}{3 n \sigma m} \sqrt{\frac{8 k T \mu}{\pi}} = 2.5 \times 10^{-6} \text{ m}^2 \text{ s}^{-1}$$

where  $\lambda$  is the mean free path of DMMP molecule in air,  $\langle U \rangle$  is the mean DMMP molecule velocity,  $n$  is the concentration of air molecules ( $2.7 \times 10^{25}\text{ m}^{-3}$ ),  $\sigma$  is the effective collision cross section ( $7.9 \times 10^{-19}\text{ m}^2$ ),  $m$  is the DMMP molecule mass

TABLE 2: Summary of Rates of Reactive Adsorption and Photocatalytic Oxidation of DMMP

characteristic	conditions			
	0.9 $\mu\text{mol}$ of DMMP		45 $\mu\text{mol}$ of DMMP	
	1% humidity	50% humidity	1% humidity	50% humidity
removal of DMMP from the gas phase	completely	completely	Reactive Adsorption up to 12 $\mu\text{mol}$	up to 4 $\mu\text{mol}$
formation of methanol	$k = 7.1 \times 10^{-2} \text{ min}^{-1}$ adsorbed only 0.9 $\mu\text{mol}$ $k = 4.2 \times 10^{-3} \text{ min}^{-1}$	$k = 5.0 \times 10^{-2} \text{ min}^{-1}$ gaseous 0.9 $\mu\text{mol}$ $k = 3.6 \times 10^{-3} \text{ min}^{-1}$	$k = 7.2 \times 10^{-2} \text{ min}^{-1}$ gaseous 1.8 $\mu\text{mol}$ $k = 2.7 \times 10^{-2} \text{ min}^{-1}$	gaseous 4.1 $\mu\text{mol}$ $k = 1.2 \times 10^{-2} \text{ min}^{-1}$
removal of DMMP from the gas phase			Photocatalytic Oxidation after Completion of Reactive Adsorption	
formation of gaseous $\text{CO}_2$	$k = 0.29 \text{ min}^{-1}$ $W_0 = 7.6 \times 10^{-7} \text{ mol min}^{-1}$	$k = 0.25 \text{ min}^{-1}$ $W_0 = 6.7 \times 10^{-7} \text{ mol min}^{-1}$	$k = 6.5 \times 10^{-3} \text{ min}^{-1}$ $k = 0.017 \text{ min}^{-1}$ $W_0 = 2.5 \times 10^{-7} \text{ mol min}^{-1}$	$k = 8.5 \times 10^{-3} \text{ min}^{-1}$ $k = 0.015 \text{ min}^{-1}$ $W_0 = 1.9 \times 10^{-7} \text{ mol min}^{-1}$
removal of DMMP from the gas phase	completely		Simultaneous Reactive Adsorption and Photocatalytic Oxidation	
formation of gaseous $\text{CO}_2$	$k = 0.28 \text{ min}^{-1}$ $k = 0.13 \text{ min}^{-1}$			

( $2.1 \times 10^{-25} \text{ kg}$ ),  $k$  is the Boltzman constant ( $1.38 \times 10^{-23} \text{ J/K}$ ),  $T$  is the temperature (300 K), and  $\mu$  is the reduced mass of DMMP and air molecules ( $3.9 \times 10^{-26} \text{ kg}$ ).

According to Einstein's law, the time of diffusion from the gas phase to the photocatalyst sample is  $t = \langle L \rangle^2 / 2D_g = 8 \text{ min}$ , where  $L$  is the characteristic length of diffusion (0.05 m for the given IR cell).

Transport of DMMP molecules inside the  $\text{TiO}_2$  sample pores obeys Knudsen's law because the pores size of the  $\text{TiO}_2$  used is  $5 \text{ nm}^{15}$  which is much smaller than the mean free path of  $30 \text{ nm}$ . The Knudsen diffusion coefficient is  $D_K = 97\rho\sqrt{T/M} = 7 \times 10^{-7} \text{ m}^2 \text{ s}^{-1}$ , where  $M$  is the molecular weight of DMMP ( $124 \text{ g mol}^{-1}$ ) and  $\rho$  is the pore diameter ( $5 \text{ nm}$ ). The characteristic time of diffusion inside the  $\text{TiO}_2$  powder film is  $t = \langle h \rangle^2 / 2D_K \sim 10^{-4} \text{ s}$ , where  $h$  is the film thickness ( $\sim 10^{-5} \text{ m}$ ).

The estimate shows that diffusion inside the  $\text{TiO}_2$  sample does not limit the removal of DMMP from the gas phase in the IR cell. The characteristic time of diffusion from the bulk gas phase to the  $\text{TiO}_2$  sample surface was estimated as 8 min which corresponds to a rate coefficient of  $0.1 \text{ min}^{-1}$ . This estimate agrees well with the measured DMMP removal rate coefficient of  $0.05\text{--}0.07 \text{ min}^{-1}$  in reactive adsorption experiments, implying that gas-phase diffusion provides the biggest DMMP removal rate limitation. For the method of simultaneous adsorption and photocatalytic oxidation, the DMMP removal rate coefficient was about 3-fold bigger than the DMMP external diffusion estimate. Since irradiation heats the photocatalyst sample, convection could provide acceleration of DMMP transport to the photocatalyst external surface.

#### IV. Conclusion

Kinetic parameters and conversion of hydrolysis and photocatalytic oxidation at all studied conditions are given in Table 2. Complete removal of gaseous DMMP was obtained for low coverage quantities only. However, an increase in humidity from 1 to 50% significantly improved the conversion. From the highest quantity of produced methanol, it is estimated that 0.68  $\mu\text{mol}$  is the maximum quantity of DMMP that can be hydrolyzed over 1 mg of given  $\text{TiO}_2$ , which corresponds to a  $0.8 \text{ nm}^2$  surface area per each adsorbed DMMP molecule.

Photocatalytic oxidation after hydrolysis of low DMMP quantities proceeds completely and an order of magnitude faster than oxidation after hydrolysis of large DMMP quantities. The fastest removal of DMMP is observed in simultaneous adsorption and photocatalytic oxidation. The rate of complete oxidation is in this case lower than that in consecutive scenarios. This can be caused by insufficient quantities of adsorbed DMMP which is consumed in oxidative reaction before accumulation over the  $\text{TiO}_2$  surface.

**Acknowledgment.** The authors thank Dr. Denis Kozlov for the help in constructing the experimental FTIR setup. We gratefully acknowledge the support of the program "Russia in Flux" via project N208134, grant NSh-1484.2003.3, NATO SFP grant 981461, and Russian Science Support Foundation.

#### References and Notes

- (1) Lin, S.-T.; Klabunde, K. J. *Langmuir* **1985**, *1*, 600–605.
- (2) Li, Y.-X.; Schlup, J. R.; Klabunde, K. J. *Langmuir* **1991**, *7*, 1394–1399.
- (3) Wagner, G. W.; Bartram, P. W.; Koper, O.; Klabunde, K. J. *J. Phys. Chem. B* **1999**, *103*, 3225–3228.
- (4) Mitchel, M. B.; Sheinker, V. N.; Mintz, E. A. *J. Phys. Chem. B* **1997**, *101*, 11192–11203.
- (5) Sheinker, V. N.; Mitchell, M. B. *Chem. Mater.* **2002**, *14*, 1257–1268.



- (6) Mitchell, M. B.; Sheinker, V. N.; Tesfamichael, A. B.; Gatimu, E. N.; Nunley, M. *J. Phys. Chem. B* **2003**, *107*, 580–586.
- (7) Cao, L.; Segal, S. R.; Suib, S. L.; Tang, X.; Satyapal, S. *J. Catal.* **2000**, *194*, 61–70.
- (8) Kanan, S. M.; Lu, Z.; Tripp, C. P. *J. Phys. Chem. B* **2002**, *106*, 9576–9580.
- (9) Kim, C. S.; Lad, R. J.; Tripp, C. P. *Sens. Actuators* **2001**, *76*, 442–448.
- (10) Rusu, C. N.; Yates, J. T. *J. Phys. Chem. B* **2000**, *104*, 12292.
- (11) Segal, S. R.; Suib, S. L.; Tang, X.; Satyapal, S. *Chem. Mater.* **1999**, *11*, 1687–1695.
- (12) Obee, T. N.; Satyapal, S. *J. Photochem. Photobiol., A* **1998**, *118*, 45–51.
- (13) Rusu, C. N.; Yates, J. T. *J. Phys. Chem. B* **2000**, *104*, 12299–12305.
- (14) Trubitsyn, D. A.; Vorontsov, A. V. *Mendeleev Commun.* **2004**, *14*, 197–199.
- (15) Vorontsov, A. V.; Savinov, E. N.; Smirniotis, P. G. *Chem. Eng. Sci.* **2000**, *55*, 5089–5098.
- (16) Vorontsov, A. V.; Davydov, L.; Reddy, E. P.; Lion, C.; Savinov, E. N.; Smirniotis, P. G. *New J. Chem.* **2002**, *26*, 732–744.
- (17) Chuang, C.-C.; Wu, W.-C.; Huang, M.-C.; Huang, I.-C.; Lin, J.-L. *J. Catal.* **1999**, *125*, 423–434.
- (18) Nakamoto, K. *Infrared and Raman Spectra of Inorganic and Coordinated Compounds*; John Wiley & Sons: New York, 1986.
- (19) Bertilsson, L.; Engquist, I.; Liedberg, B. *J. Phys. Chem. B* **1997**, *101*, 6021.
- (20) Vorontsov, A. V.; Savinov, E. N.; Davydov, L.; Smirniotis, P. G. *Appl. Catal., B* **2001**, *32*, 11–24.